Available online at www.sciencedirect.com
SCIENCE DIRECT®
Physics of the Earth and Planetary Interiors 154 (2006) 308–322
PHYSICS OF THE EARTH AND PLANETARY INTERIORS
www.elsevier.com/locate/pepi

# First-order reversal curve (FORC) diagrams of magnetic mixtures: Micromagnetic models and measurements

Claire Carvallo[a,c,*], Adrian R. Muxworthy[b,c], David J. Dunlop[a]

[a] *Geophysics, Physics Department, University of Toronto at Mississauga, Mississauga, Ont., Canada L5L1C6*
[b] *School of GeoSciences, University of Edinburgh, King's Buildings, West Mains Road, Edinburgh EH9 3JW, UK*
[c] *School of Ocean and Earth Science, University of Southampton, National Oceanography Centre, European Way, Southampton SO14 3ZH, UK*

Received 22 November 2004; received in revised form 1 April 2005; accepted 7 November 2005

**Abstract**

First-order reversal curve (FORC) diagrams were modelled and experimentally measured for different assemblages of single-domain (SD) magnetite particles with bimodal distributions of coercivities, and varying concentrations. When fitting end-member FORC diagrams to the FORC diagrams of mixtures, linear additivity is obeyed for the non-interacting mixtures, with predicted mixing ratios within the errorbars of the actual mixing ratios. Interacting mixtures are not always linearly additive. Experimental bimodal mixtures of magnetite particles (SD + pseudo-single-domain, PSD) have FORC diagrams that are usually linearly additive, regardless of the magnetite concentration of the sample (10 or 1%). Measured FORC diagrams of mixtures of SD magnetite and SD hematite again show that linear additivity of the two end-members holds. However, the very small $M_s$ of hematite compared to that of magnetite makes it difficult to detect a contribution on a FORC diagram from hematite, unless it comprises at least 88% of the mixture.
© 2006 Elsevier B.V. All rights reserved.

*Keywords:* FORC diagram; Interactions; Micromagnetic model; Magnetic mixtures; SD magnetite

## 1. Introduction

Natural samples usually contain mixtures of magnetic minerals in various domain states. An accurate identification of the magnetic minerals and their domain states is necessary in many studies in palaeomagnetism or environmental magnetism. For example, the reliability of palaeomagnetic recording is strongly dependent on grain size and domain structure. However, mixtures greatly complicate magnetic signals, and magnetic interactions between grains introduce additional complexity. In non-interacting assemblages, the magnetizations of different phases are linearly additive (Roberts et al., 1995). In assemblages with magnetostatic interactions, linear additivity is more controversial. Lees (1997) demonstrated non-linearity of magnetization as a function of mixing ratio, while Carter-Stiglitz et al. (2001) found linear additivity in their samples.

In this paper we investigate the effect of mixtures on first-order reversal curve (FORC) diagrams. FORC diagrams, introduced in rock magnetism by Roberts et al. (2000), provided a new way of identifying minerals and domain states by measuring partial hysteresis curves. The measurement of a FORC diagram begins by magnetically saturating the sample. The field is then decreased to a field $H_a$ and increased again up to saturation through field steps $H_b$. This process is repeated for

* Corresponding author. Present address: Institut de Minéralogie et de Physique des Milieux Condensés, Université Pierre et Marie Curie, Paris, France. Tel.: +33 1 44 27 52 27.
*E-mail address:* carvallo@impmc.jussieu.fr (C. Carvallo)

0031-9201/$ – see front matter © 2006 Elsevier B.V. All rights reserved.
doi:10.1016/j.pepi.2005.06.017

about 100 different values of $H_a$. The FORC distribution is defined by

$$\rho(H_a, H_b) = -\frac{\partial^2 M(H_a, H_b)}{\partial H_a \partial H_b} \quad (1)$$

where $M(H_a, H_b)$ is the magnetization measured at $(H_a, H_b)$. A FORC diagram is a contour plot of $\rho(H_a, H_b)$ along 45° rotated axes ($H_c = (H_b - H_a)/2$, $H_u = (H_b + H_a)/2$). The FORC distribution $\rho(H_a, H_b)$ at a point $P$ is calculated by fitting a polynomial surface on a local square grid with $P$ at the centre (Pike et al., 1999; Roberts et al., 2000). The smoothing factor (SF) sets the size of the local square grid on which the polynomial fit of the magnetization is performed. The number of points on the grid is $(2SF + 1)^2$.

Since FORC diagrams are able to reveal the coercive force distribution as well as the magnetic interactions within an assemblage (Stancu et al., 2003; Carvallo et al., 2004; Muxworthy and Williams, 2005), they should provide a good method of identifying individual minerals in magnetic mixtures. A few FORC diagrams of bimodal grain-size distributions and assemblages of different magnetic minerals in both natural and synthetic samples have been reported (Roberts et al., 2000; Weaver et al., 2002; Muxworthy et al., 2005). However, before routinely using FORC diagrams to analyse magnetic mixtures, we must investigate the effects of mixtures on FORC diagrams. We have taken a micromagnetic modelling approach to better understand the response of interacting and non-interacting assemblages of single-domain grains on a FORC diagram. We have also measured FORC diagrams for a series of mixtures of magnetites with bimodal grain-size distributions, as well as mixtures of magnetite and hematite.

Hysteresis loops have been used widely to identify minerals in magnetic mixtures. Bimodal mixtures are often characterized by loops with a constricted middle ("wasp-waists") (Roberts et al., 1995) or by a spreading middle and slouching shoulders ("potbellies") (Tauxe et al., 1996). Measurements and simulations have indicated that single-domain (SD)/superparamagnetic (SP) mixtures can readily produce wasp-waisted and potbellied loops. Mixtures of two minerals, one magnetically soft (magnetite or maghemite, for example) and one magnetically hard (like hematite or goethite) can also produce wasp-waisted loops, provided the two phases contribute comparable amounts of magnetization.

Hysteresis parameters give some indication of the domain state of the dominant magnetic mineral. However, there is strong evidence that hysteresis parameters can give ambiguous results, because variations in internal stress, grain interactions, mineral composition and grain size can yield similar hysteresis parameters (Dunlop, 2002; Muxworthy et al., 2003). Thermomagnetic curves or susceptibility variations with temperature can often identify individual magnetic minerals, provided that the ranges of Curie points do not overlap. Phase transitions at low temperature (Verwey transition at ∼120 K for magnetite, Morin transition at ∼258 K for hematite, pyrrhotite at 30–34 K) are also useful for identifying these minerals. Magnetic granulometry techniques usually provide only a measure of the average mineral magnetic properties in a sample and tend to break down when a sample contains a mixture of grain sizes (Day et al., 1977). Mixtures of grains of different sizes can be detected in several ways. For example, large SP grains can be detected by measuring the frequency dependence of magnetic susceptibility (Bloemendal et al., 1985). This method might not work for sediment and soil samples, where the paramagnetic contribution to the total low-field susceptibility can be considerable so that calculating frequency dependence may yield aberrant numbers. Low-temperature demagnetization (cooling below the isotropic point and Verwey transition of magnetite and warming up to room temperature in zero field) can be helpful in estimating the domain state. The remanence of multidomain (MD) magnetite grains will be preferentially demagnetized during low-temperature treatment, while SD grains are largely unaffected (Dunlop and Argyle, 1991). This method allows one to discriminate between mixtures of SD + SP and SD + MD magnetite, because SP grains do not contribute to the remanence.

In this study, we examine the ability of FORC diagrams to predict the proportion of each end-member in a mixture. We inversely numerically fit the reversal curves of each mixture by a linear combination of the reversal curves (FORCs) of the end-members in various proportions to the mixed FORC data using a linear least-squares algorithm. If the predicted proportion is identical to the actual proportion, then linear additivity is obeyed. The unmixing algorithm based on linear additivity could work well at predicting the proportions even in the presence of non-linear mixing. However, in this paper we are interested in the unmixing power of FORC diagrams that could be used to identify and quantify magnetic minerals in natural assemblages, so this definition of linear unmixing is appropriate for this study. The same unmixing method is used to investigate the predictive power of major hysteresis loops, in order to determine which measurement (FORC diagram or major hysteresis loop) gives the best estimate of end-member proportion. The quality of the fit was tested using a bootstrap without replacement algorithm (Efron and Tibshirani, 1993).

## 2. Micromagnetic models

In order to model large arrays of particles, the grains are assumed to be perfectly single-domain, i.e., there is no variation of magnetization within a grain and each grain can then be represented by one magnetic moment. Mixtures of magnetites with two different coercivities and mixtures of magnetite and hematite were modelled. The micromagnetic model used here is described by Wright et al. (1997). A conjugate gradient algorithm minimizes the total energy of the model grain, which is the sum of the magnetostatic self-demagnetizing energy $E_d$, the anisotropy energy $E_{anis}$ and the external field energy $E_h$. The computing time is reduced by using a fast-Fourier transform algorithm. To model magnetite, the anisotropy is uniaxial and the saturation magnetization $M_s$ is $480\,kAm^{-1}$ (Pauthenet and Bochirol, 1951) and $K_1 = 1.25 \times 10^4\,Jm^{-3}$ (Fletcher and O'Reilly, 1974). In mixtures of magnetite with a bimodal coercivity distribution, one population has $K_1 = 1.25 \times 10^4\,Jm^{-3}$, and the second population has $K_1$ chosen between 0.3 and $1 \times 10^4\,Jm^{-3}$. Even though $K_1$ is changed, the other parameters are kept constant, so we are still dealing with magnetite, but it behaves like an ensemble of elongated grains rather than equidimensional grains. This range of $K_1$ values corresponds to coercivities ranging from 8 to 27 mT.

The spacing between the grains can be adjusted; this permits modelling of different levels of interactions in the assemblage (Muxworthy et al., 2003). Interaction spacing is expressed as $d$, the distance between grains, divided by grain dimensions. Each value of $d$ can be translated in a magnetite concentration. Based on micromagnetic calculations, grains interact significantly if the spacing between them is smaller than one grain width (Muxworthy et al., 2003). Micromagnetic modelling of FORC diagrams for small arrays of magnetite particles showed that the effect of interactions is visible on a FORC diagram if the spacing between particles is less than about twice the distance between particles (Carvallo et al., 2003). The value of $d$ where the interaction effects become visible depends on the anisotropy symmetry, because the amount of spreading of the main peak depends on the anisotropy. At identical spacing, the spreading of the main peak of the FORC distribution is larger for grains with cubic anisotropy than for grains with uniaxial anisotropy (Muxworthy et al., 2004).

## 3. Modelled mixtures of magnetite

We used arrays of $8 \times 8 \times 8$ (512) grains to model mixtures of magnetite having a bimodal coercivity distribution. This size is large enough, since Muxworthy et al. (2004) found little variation in behaviour between assemblages of 216 and 8000 grains.

FORC diagrams were modelled for five different bimodal mixtures: M1 (28 mT) with M2 (22 mT), M3 (18 mT), M4 (14 mT), M5 (11 mT) and M6 (8 mT). If the grains were non-equidimensional, the variations in coercivity could be translated into variations in elongation. Assuming that effective shape anisotropy is the only cause of anisotropy, elongation ratios would range between 1.09 and 1.22 (Dunlop and Özdemir, 1997). For each bimodal mixtures, four different compositions were modelled. In order to determine the coercivity of a particular grain in the array, a random number between 0 and 1 was picked for each grain. The bimodal assemblages modelled are composed of 20% of A, 80% of B; 40% of A, 60% of B; 60% of A, 40% of B; or 80% of A, 20% of B. For the model assemblages of non-interacting randomly oriented uniaxial SD grains, the ratios $M_{rs}/M_s$ are between 0.48 and 0.50, in good agreement with the theoretical value of 0.5 (Stoner and Wohlfarth, 1948). The field spacing for the simulated FORCs for all the magnetite mixtures is 1.24 mT. Close to the $H_c = 0$ axis, the grids are incomplete because smoothing involves extrapolation of the FORC distribution. The corresponding areas of the FORC diagram are therefore hatched.

### 3.1. Non-interacting mixtures ($d = 5$)

An inter-grain spacing of five corresponds to a magnetite concentration of 0.6%. Micromagnetically modelled FORC diagrams for an array of non-interacting uniform SD particles having the same size (therefore the same coercivity) are characterized by a single peak centered at ($H_u = 0$, $H_c$). The FORC diagrams of non-interacting mixtures were all calculated with a SF of three. Fig. 1 is an example of bimodal combinations. The presence of two different coercivities is apparent in each case, and the progression from the first end-member to the second can be seen clearly.

### 3.2. Interacting mixtures ($0.5 \leq d \leq 3$)

The FORC diagrams for four different mixtures of M1 and M3 with spacings of 1.5 and 1 (4.8 and 15% magnetite concentrations, respectively) are plotted in Figs. 2 and 3, respectively. The FORC distributions of interacting mixtures are much noisier than those of non-interacting mixtures, and the noise level increases with decreasing spacing. When $d$ is 1 or less, the well-defined coercivity peaks disappear and FORC distributions are dominated by noise (Fig. 3).

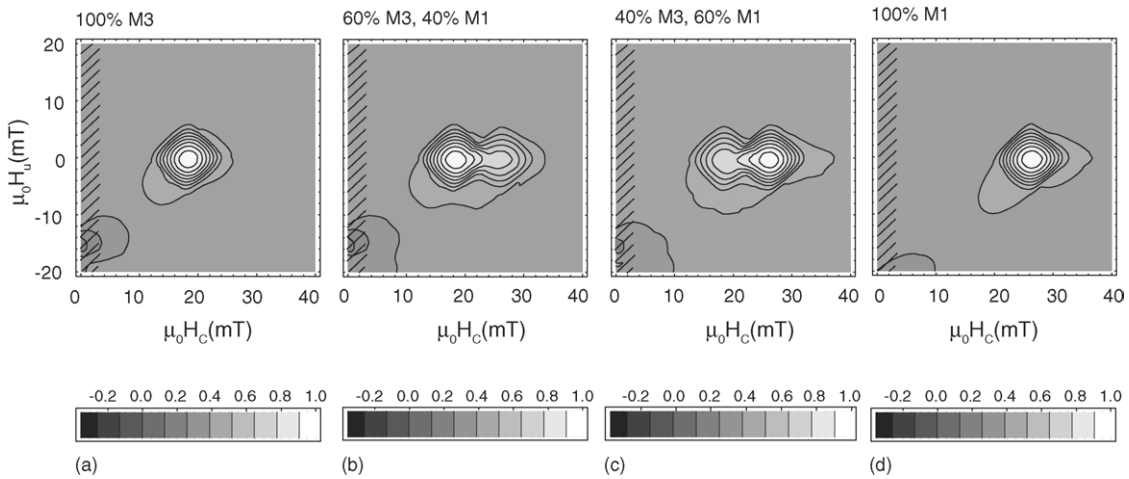


Fig. 1. Modelled FORC diagrams for different non-interacting mixtures of M1 and M3, containing 512 grains, $d = 5$, corresponding to a concentration of 0.6%. (a) 100% M3; (b) 60% M3, 40% M1; (c) 40% M3, 60% M1; (d) 100% M1, SF = 5.

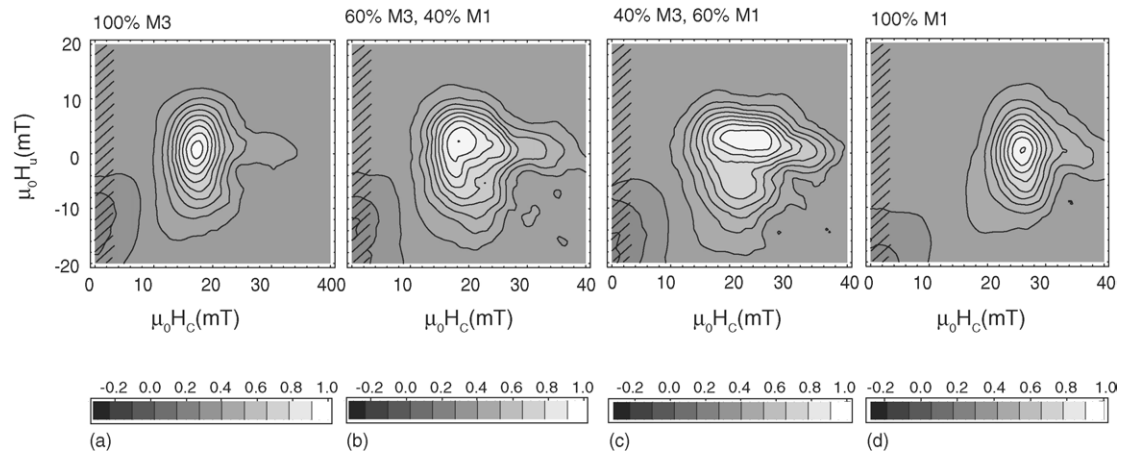


Fig. 2. Modelled FORC diagrams for different interacting mixtures of M1 and M3, containing 512 grains, $d = 1.5$, corresponding to a concentration of 4.8%. (a) 100% M3; (b) 60% M3, 40% M1; (c) 40% M3, 60% M1; (d) 100% M1, SF = 5.

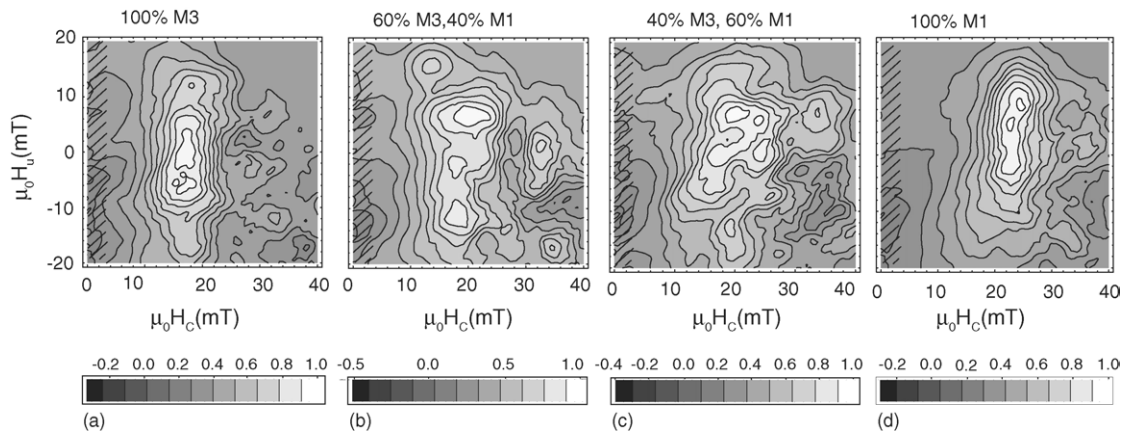


Fig. 3. Modelled FORC diagrams for different interacting mixtures of M1 and M3, containing 512 grains, $d = 1.0$, corresponding to a concentration of 15%. (a) 100% M3; (b) 60% M3, 40% M1; (c) 40% M3, 60% M1; (d) 100% M1, SF = 5.

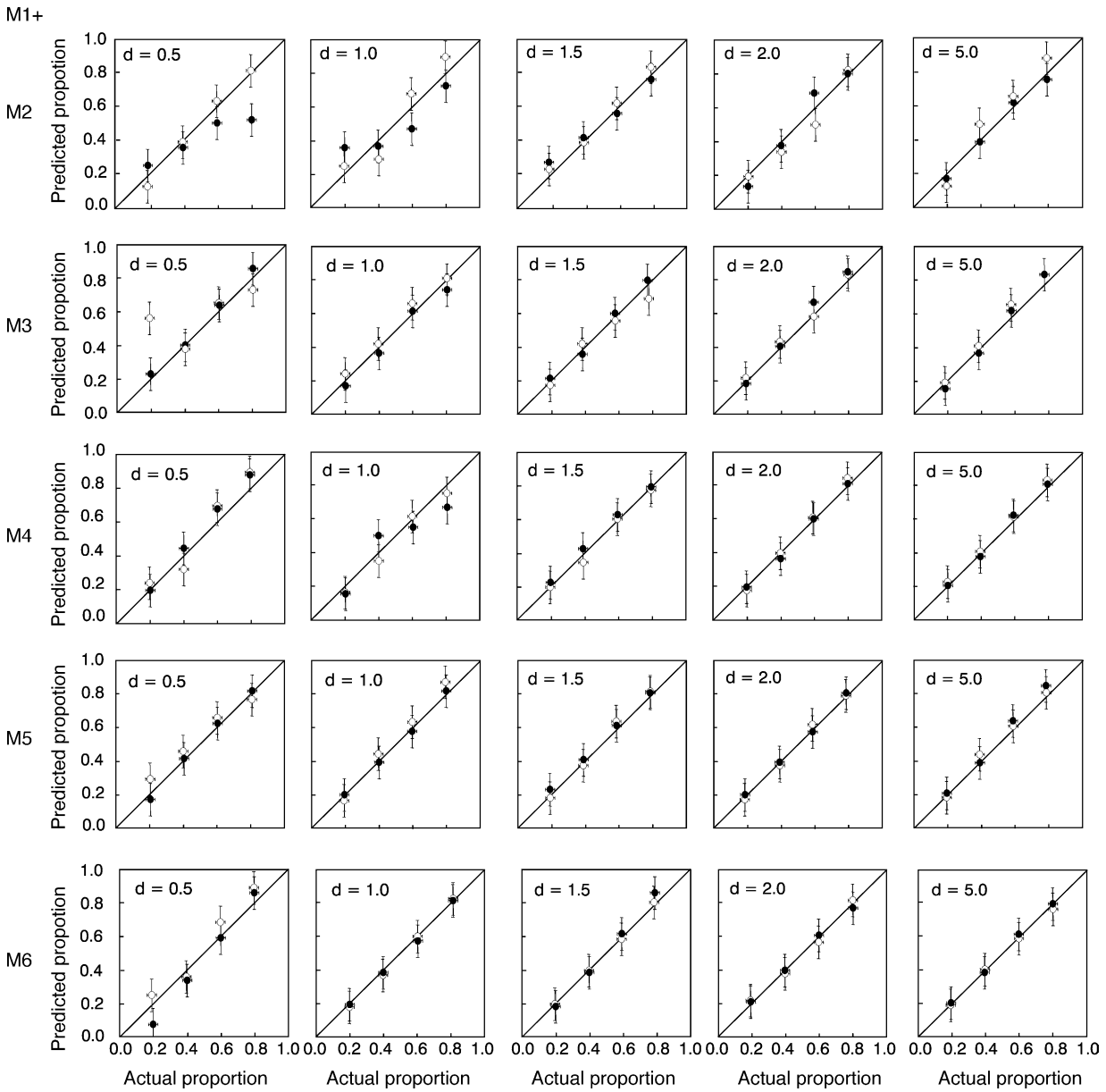


Fig. 4. Predicted proportion of one end-member (M1) vs. that in the actual mixture of M1 + M2 to M1 + M6, for various spacings between particles. The predicted proportions were obtained by linearly fitting: closed circles, end-member FORCs to the mixed-sample FORC; open circles, end-member major hysteresis loops to the mixed-sample hysteresis loops. The $y = x$ line represents linear additivity.

Increasing the interactions (i.e., reducing $d$ from 5 to 2) causes the coercivity peaks to widen in the $H_u$ direction (Figs. 2 and 3). The width of the coercivity is measured by calculating the full-width at half maximum (FWHM) of the peak. For example, with identical SF, an assemblage of non-interacting M1 ($d = 5$) has a FWHM of only 12.5 mT on the $H_c$ axis and 12 mT on the $H_u$ axis, whereas the main peak of an interacting assemblage ($d = 1.5$) still has a FWHM of 12.5 mT on the $H_c$ axis, but almost 25 mT on the $H_u$ axis. This is consistent with model and experimental evidence that spreading along the $H_u$ axis indicates the presence of magnetostatic interactions (Pike et al., 1999; Roberts et al., 2000). The spread on the $H_u$ axis drops sharply when $d$ is increased from 1.5 to 2, and then more smoothly when $d$ is further increased to 3. Increasing $d$ even more does not change the spread.

### 3.3. Linear fitting

Actual proportions of one end-member versus the predicted proportions of the same end-member from the end-member fitting are shown in Fig. 4 for the 25 different mixtures. Errors in both the actual and predicted proportions that are shown in the error bars in Fig. 4 have various origins.

Error in the actual proportions: the actual proportion of each component in a mixture is calculated by picking random numbers, so there is an error in the proportion itself. By replicating the random number selection process in an array of 512 grains, the actual proportions of the mixture were found to deviate no more than 3% from the target proportions. Therefore, the error in the actual proportions is estimated to be $\leq$3%.

Error in the predicted proportions from the fitting process: the errors in the fits are small because of the large number of data points used for each fit (more than 6000 for only one parameter). However, the standard deviations of the fits are about 10 times larger when the particles in the mixtures are interacting than when they are not. This error is still at least three orders of magnitude smaller than the discrepancies between predicted and actual mixture proportions.

Error in the predicted proportions from the randomness of the assemblages: an important error in the fitted proportions comes from the random nature of the grain orientation in the assemblage. The array is relatively small (512 grains), so there will be some variation in the predicted proportions of end-members when a different set of grain orientations is used. This error is difficult to estimate. We recalculated FORC diagrams for each of the end-members using a set of grain orientations different from the orientations used previously. Then we fitted the mixture FORC diagrams using these new end-members. Differences in predicted proportions ranged from 2 to 8%. Therefore, we chose 8% as an estimate of error in the predicted proportions. This is quite large, and could be decreased by increasing the size of the modelled assemblages, but the computation time would then increase significantly by $N \log N$, where $N$ is the total number of grains.

Linear additivity holds quite well for all the mixtures of weakly interacting and non-interacting grains ($d \geq 1.5$): the predicted proportions are always within 8% of the actual proportions. Highly interacting mixtures ($d = 1.0$ or $0.5$) do not obey linear additivity as well, in particular the mixture of M1 and M2, which have very close coercivities (28 and 22 mT, respectively). However, other mixtures such as M1 + M3 and M1 + M5 still give predicted proportions that are within 7% of the actual proportions.

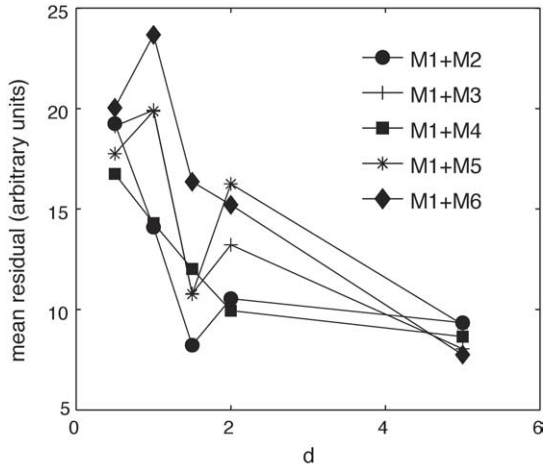


Fig. 5. Residuals from the FORC best fits as a function of the spacing between grains, for the five modelled mixtures.

For interacting mixtures, interactions nevertheless do have a visible effect on the FORC diagrams of the mixtures. The low-$H_c$ component remains more important than simple linear superposition of FORCs would predict (e.g., Fig. 2c). Our linear additivity procedure only tests whether it is possible to unmix and get approximately the correct proportions, within 8%. This is also evident in the variation of the residuals from the fits as a function of $d$ (Fig. 5). Residuals for the non-interacting mixtures ($d = 5$) are always smaller than for interacting mixtures ($d < 1$).

### 3.4. Linear fitting of major hysteresis loops

In order to test whether FORC diagrams predict compositions better than major hysteresis loops, linear additivity of the major hysteresis loops was also tested, using the same method as for the FORCs (Fig. 4). The error in the actual proportions is still $\leq$3%. By repeating the fitting using different random orientations of the grains in the end-member assemblages, we again found differences up to 8%. In general, predicted proportions of end-members follow the trend of the actual proportions fairly closely, but not as closely as the proportions predicted from FORC fitting. For highly interacting mixtures ($d = 0.5$ and 1.0), the predicted proportions for major loops are sometimes in error by as much as 12%.

The sum of the residuals from all the fitting is 5% higher for the fits from major loops than for the FORCs. However, for the non-interacting or weakly interacting mixtures ($1.5 \leq d \leq 5$), all the proportions predicted from fitting the end-member FORC diagrams give the

correct proportions within the error bars. When fitting the end-member major loops, the predicted proportions are wrong for four mixtures out of 60. In strongly interacting mixtures, the predicted proportions are wrong for seven out of 40 mixtures according to FORC linear additivity, and five out of 40 mixtures according to major hysteresis loop additivity. FORCs are better at predicting proportions than major hysteresis loops when interactions are not too strong ($d \geq 1.5$). This result was expected, since FORC diagrams are based on two orders of magnitude more data points than major hysteresis loops.

## 4. Experimental measurements of FORC diagrams for magnetic mixtures

### 4.1. Samples

#### 4.1.1. Magnetite samples

Measurements of magnetite mixtures were carried out using an alternating gradient magnetometer at the University of Toronto. The maximum field was 0.5 T, enough to saturate magnetite. The three synthetic magnetites used as end-members to make mixtures were Wright magnetites M4000, M5000, and M112978. A grain-size characterization by scanning electron microscopy gives the following grain size arithmetic means and elongations mean $q$ (Yu et al., 2002): $0.07 \pm 0.04$ μm ($q = 1.5 \pm 0.4$) for M4000; $0.3 \pm 0.2$ μm ($q = 1.7 \pm 0.6$) for M5000 and $0.4 \pm 0.2$ μm ($q = 1.3 \pm 0.3$) for M112978. The samples were not stored in a desiccator, therefore they are likely to have oxidized.

The mixtures were made by combining the end-members in prescribed mass percentages (measured with a five-digits microbalance) and dispersing them in non-magnetic $CaF_2$. Typical masses involved are around a few milligrams. An error in the mass percentages can occur in the process, because some material may be lost when transferring the powders, and also because the mixture may not be perfectly homogeneous. Each mixture was made with two different magnetic concentrations within the $CaF_2$ matrix (10 and 1%), with the intention of studying the effect of interactions on the additivity. We measured FORC diagrams for mixtures of M4000 and M5000, M4000 and M112978, and M5000 and M112978, each with two different magnetic concentrations. The concentration differences did not have any discernible effect on the FORC distributions. This is probably because it is difficult to make non-interacting samples: the magnetic grains always have a tendency to cluster together and it is difficult to disperse them uniformly in the $CaF_2$ matrix (e.g., van Oorschot and Dekkers, 1999).

#### 4.1.2. Hematite samples

Hematite was produced by oxidizing the magnetite powders M4000 and M5000. The magnetite was heated at 700 °C in air for 4–5 h. Before making the mixtures, we measured SIRM cooling curves of hematite samples from room temperature to 20 K. The Morin transition at around 258 K is caused by hematite, whereas the Verwey transition and the isotropic point at about 130 K indicate the presence of magnetite. Only samples showing a clear Morin transition and no trace of a Verwey transition (caused by magnetite that has not been oxidized) were used in the mixtures. The magnetite-hematite mixtures were not dispersed in CaF.

We measured cooling and warming curves of saturation isothermal remanent magnetization (SIRM) for some of the mixtures (e.g., mixtures of M5000 magnetite and hematite produced by oxidizing the M5000 magnetite; Fig. 6). Both the Morin transition and the Verwey transition should be present. When magnetite is added to the original hematite sample, the Verwey transition appears in both the low-temperature warming curve of SIRM (20 K) and the low-temperature cooling and warming of SIRM (300 K). The Morin transition is still clear (in particular in the SIRM (300 K) cooling curve) even when magnetite constitutes as much as 10% of the mixture. If more magnetite is added to the mixture, the Morin transition can still be detected as a slight hump in the SIRM (300 K) cooling curve (e.g. 50–50 mixture).

### 4.2. Bimodal mixtures of magnetite

#### 4.2.1. End-member FORC diagrams

We first measured FORC diagrams for each of the end-members. Hysteresis parameters are shown in Table 1. M5000 has a FORC distribution characteristic of small PSD grains (cf. Roberts et al., 2000), with closed innermost contours and outermost contours that intersect the vertical axis (Fig. 7a). The spreading parallel to the vertical axis indicates significant magnetostatic interaction. M4000 has an SD-like FORC diagram, with most of the contours closing on the diagram, with magnetostatic interactions (Figs. 7e and 8a). Finally, the FORC distribution of M112978 indicates a PSD grain size (Fig. 8e), larger than that of M5000. The contours diverge toward

Table 1
Magnetic hysteresis parameters for the synthetic magnetite samples, diluted at 10% in CaF

| Magnetite name | $M_{rs}/M_s$ | $\mu_0 H_c$(mT) | $\mu_0 H_{cr}$(mT) |
|---|---|---|---|
| M5000 | 0.327 | 16.80 | 27.16 |
| M4000 | 0.440 | 35.12 | 42.10 |
| M112978 | 0.101 | 9.76 | 28.59 |

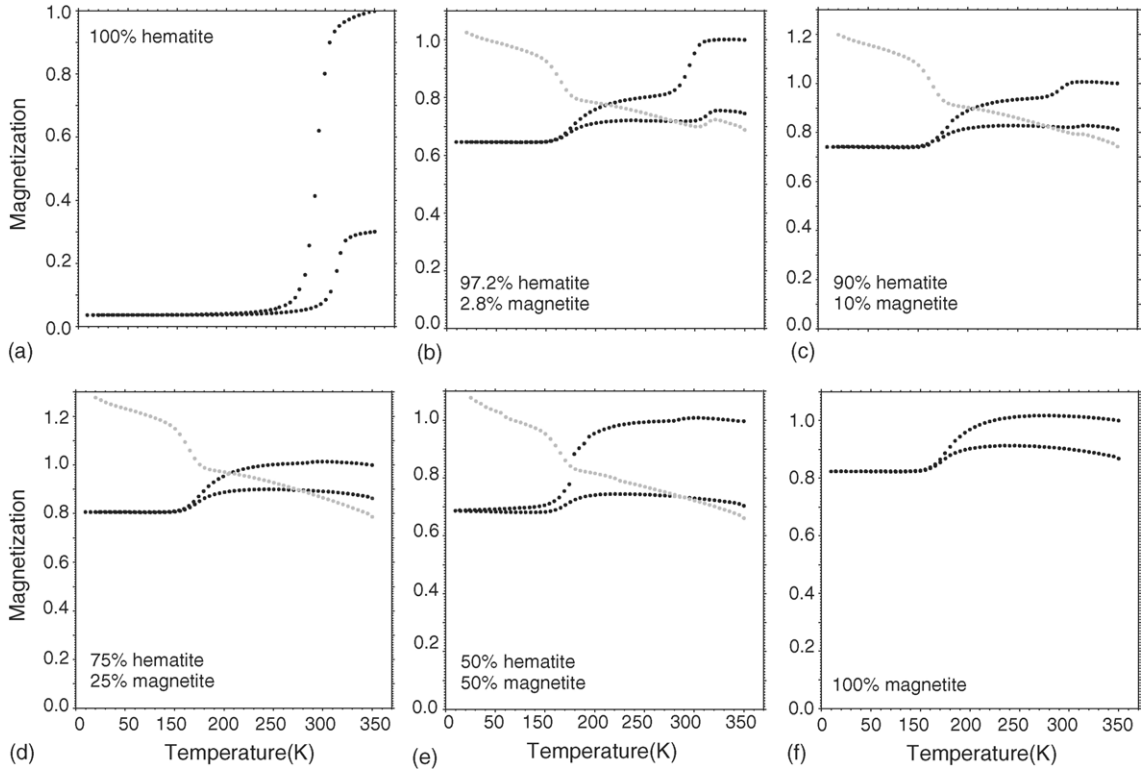


Fig. 6. Temperature dependence of SIRM produced with a 2.5 T field for undiluted end-members and mixtures of magnetite and hematite. Grey circles: warming curve from 20 to 300 K for a zero-field SIRM produced at 20 K. Black circles: zero-field cooling (300–20 K) and warming curves for SIRM produced at 300 K.

the vertical axis more than for the FORC diagram of M5000 (Fig. 7a).

### 4.2.2. FORC diagrams of mixtures

The FORC distributions for the mixtures of M5000 and M4000 clearly progress from a PSD-like pattern to a more SD-like pattern (Fig. 7). The coercivity peak that is close to the vertical axis for M5000 moves toward higher coercivities, and the FORC distribution becomes more and more spread out when M4000 is added to the mixtures. The progressive shift from one end-member to the other is also apparent in the mixtures of M4000 and M112978 (Fig. 8). The coercivity contrast between the two end-members is larger than in the mixture of M4000 and M5000. In Fig. 8c, the two coercivity peaks appear separately on

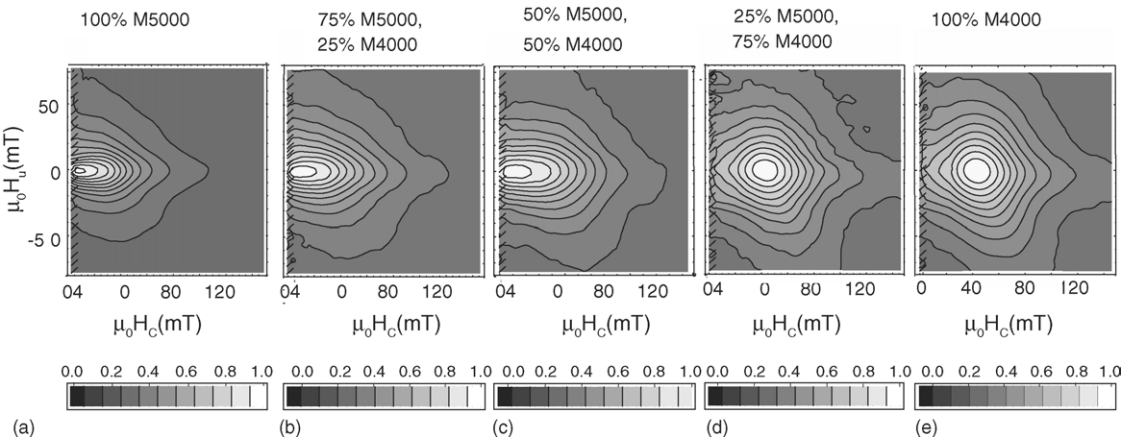


Fig. 7. Series of FORC diagrams showing measured mixtures of magnetites M5000 and M4000, SF = 3.

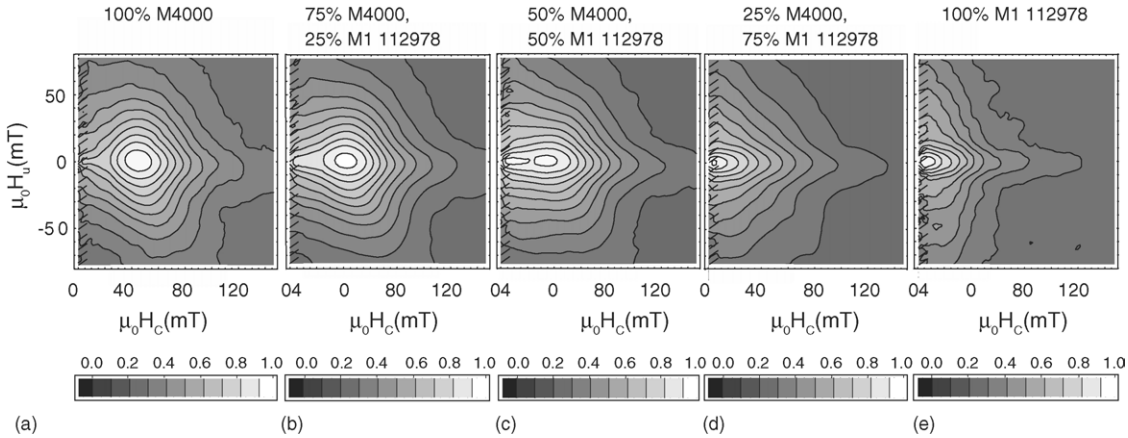


Fig. 8. Series of FORC diagrams showing measured mixtures of magnetites M4000 and M112978, SF = 3.

the FORC diagram of the mixture with 50% of each end-member.

*4.2.3. Linear fitting*

The ability of FORC diagrams to predict the correct proportions of each end-member is tested by fitting linearly each mixture to the end-member FORCs (Fig. 9). The error in initial proportions of the mixtures is estimated to be ±5%. There is a larger error in the end-member FORCs themselves, because of the possible non-homogeneity of the end-members. In order to estimate this error we re-measured FORC diagrams for new samples of each end-member and fitted the mixture FORCs to the re-measured end-member FORCs. The difference between the two fits is between 2 and 5% for the 10% concentration mixtures, and between 6 and

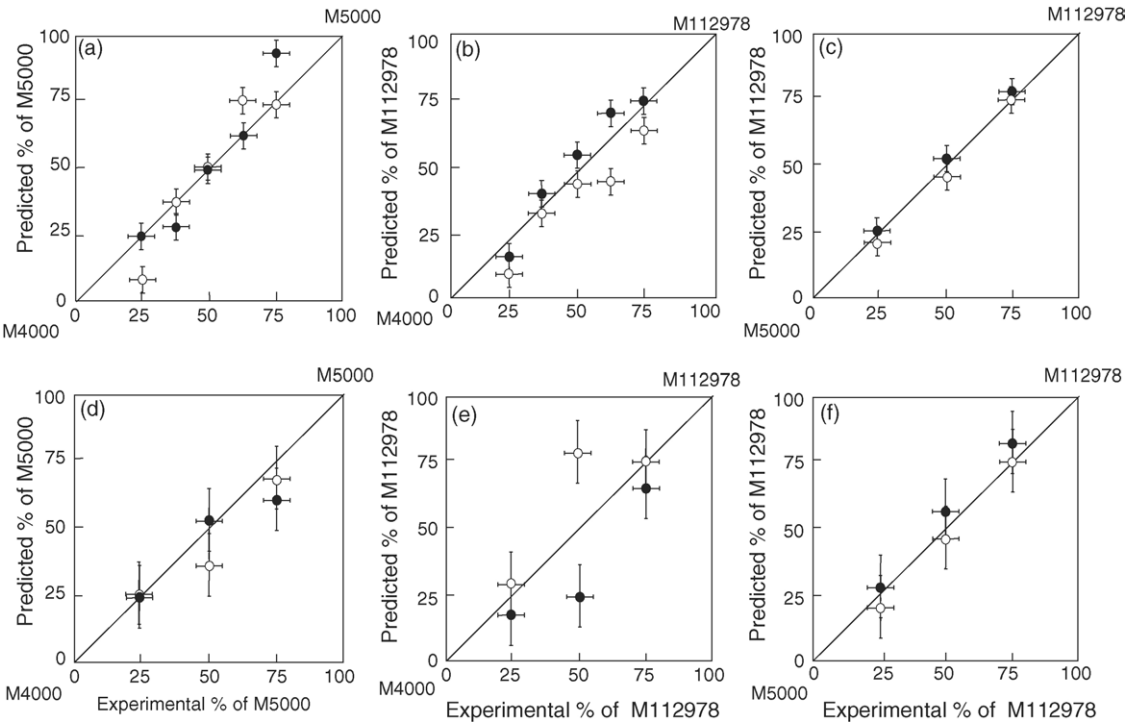


Fig. 9. Predicted percentage of M5000(a and d) or M112978(b, c, e, and f) mixed with M4000 or M5000 vs. that in the actual sample. The $y = x$ line represents ideal linear additivity. The predicted percentages were obtained by linearly fitting: closed circles, end-member FORCs to the mixed sample FORC; open circles, end-member hysteresis loops to the mixed sample hysteresis loop. Top row: 10% concentration; bottom row: 1% concentration.

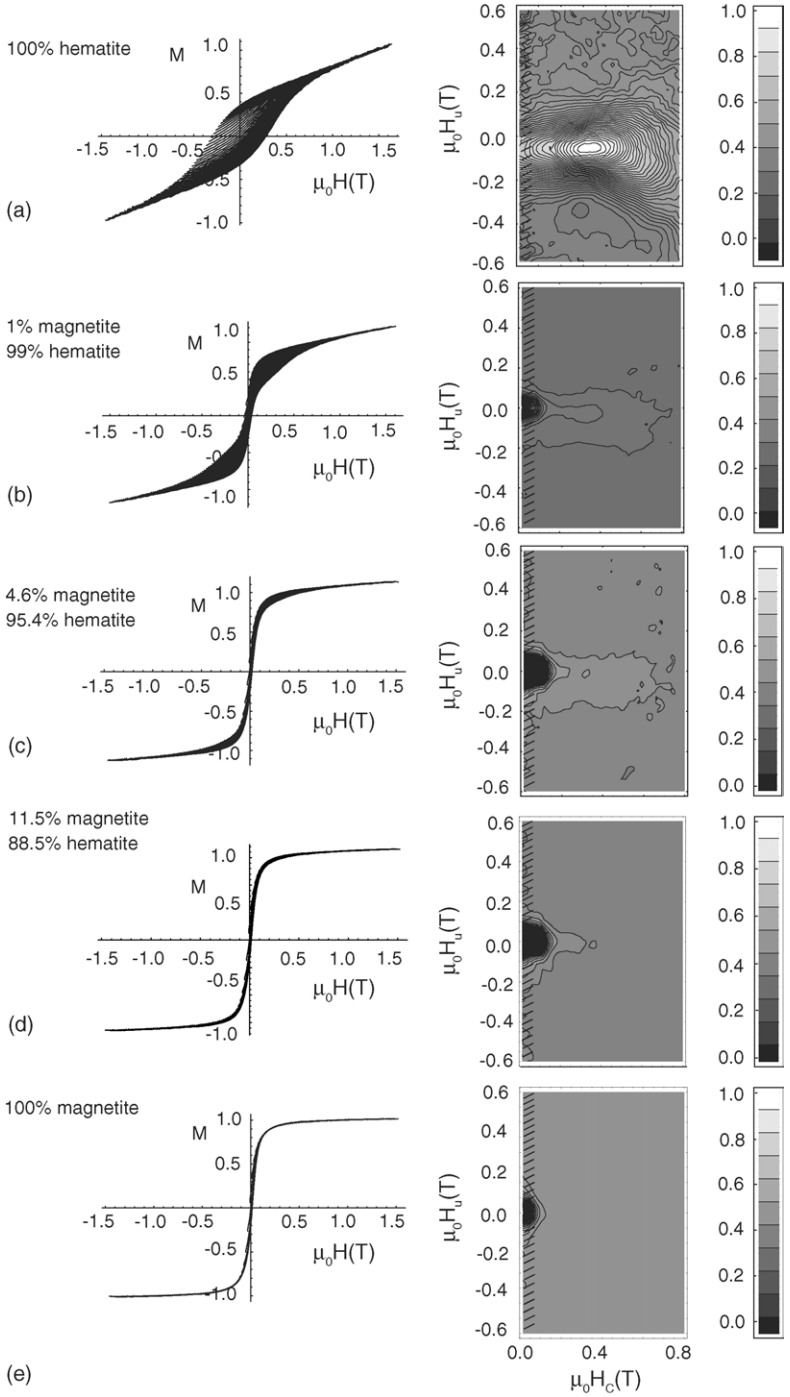


Fig. 10. Measured FORCs (left column) and FORC diagrams (right column) of an mixture of M4000 magnetite and hematite made from M4000 magnetite. The number of contours on the FORC diagrams had to be increased compared to the other FORC diagrams shown in this paper, in order to indicate the hematite peak. (a) 100% hematite; (b) 99% hematite, 1% magnetite; (c) 95.4% hematite, 4.6% magnetite, (d) 88.5% hematite, 11.5% magnetite; (e) 100% magnetite, SF = 5.

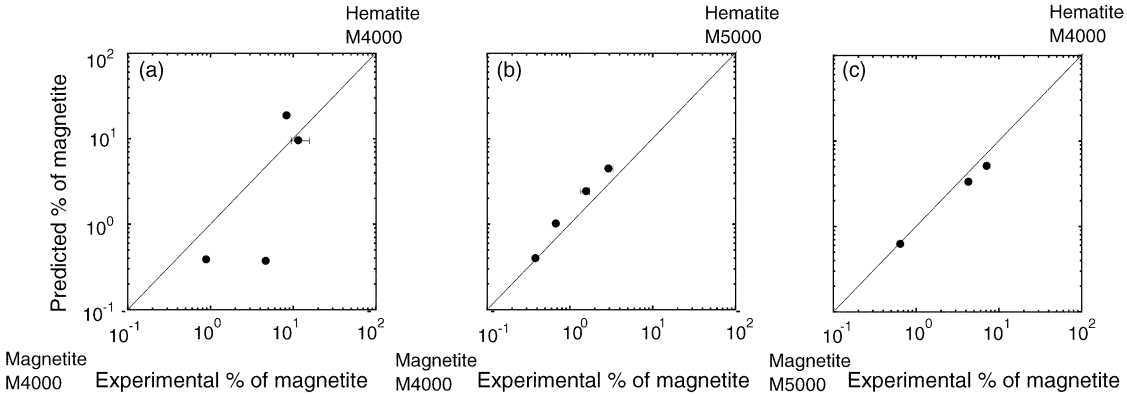


Fig. 11. Predicted percentage of magnetite mixed with hematite vs. that in the actual sample. End-members are: (a) magnetite M4000 and hematite made from M4000; (b) magnetite M4000 and hematite made from M5000; (c) magnetite M5000 and hematite made from M4000. The $y = x$ line represents ideal linear additivity.

12% for the 1% concentration mixtures. The larger error in the 1% mixtures was expected, because it is more difficult to accurately measure proportions and to make a homogeneous sample in a less concentrated mixture. Therefore, errors on the fits are estimated to be $\leq$5% for the 10% concentration mixtures and $\leq$12% for the 1% concentration mixtures.

Only three proportions predicted from the linear fitting to the end-members are more than 5% different from the actual proportion, and only one is more than 8% different. The 1% concentration mixtures do not show such good agreement. This is probably because it is more difficult to do accurate mass measurements with such small quantities of magnetite.

Predicted proportions roughly follow the trend of the actual proportion in the mixtures for major loops, but agreement with the actual proportions is not as good as it is when using FORC diagrams (Fig. 9). FORCs fail to predict the correct proportions in five mixtures out of 22, and predictions from major hysteresis loops fail in seven mixtures out of 22. Moreover, the sum of the residuals from all the fittings is 40% higher for the major loop fitting than for the FORC fitting. These results show that FORC diagrams can predict end-member proportions better than major hysteresis loops.

### 4.3. Assemblages of magnetite and hematite

#### 4.3.1. FORC diagrams

FORC diagrams of mixtures of hematite and magnetite were measured at the Institute for Rock Magnetism (University of Minnesota). Examples of FORC diagrams for a set of mixtures of hematite and magnetite, as well as the FORC diagrams for the end-members, are shown in Fig. 10. The FORC distribution of hematite is characterized by a broad peak centered at a large coercivity (around 400 mT). This pattern is consistent with other measurements of FORC diagrams on hematite (Muxworthy et al., 2005).

Additional contours had to be plotted on the FORC diagrams compared to the number routinely used in order to see the pattern created by the hematite in the mixtures. If we did not know that hematite was present in the sample, it would not have been possible to detect it using the standard FORC processing routine. It could be argued that the hematite is more easily visible on the hysteresis loop than on a normal FORC diagram (usually with 10 contours) but in the mixtures containing more than 5% magnetite, the hematite would also have been missed on the hysteresis loops if the saturation field were not large enough. Moreover, if the identity of the low $M_s$ component were not known, it would be difficult to differentiate hematite from another low $M_s$ mineral only on the basis of a high coercivity lobe as small as that in Fig. 10d.

#### 4.3.2. Linear fitting

When linearly fitting FORCs of the mixtures to those of end-members, FORCs have to be weighted with respect to $M_s$. For pure magnetite and pure hematite, $M_s = 92$ and $0.3\,\mathrm{Am^2/kg}$, respectively. All of the magnetite samples had a clear Verwey transition, and all of the hematite samples had a clear Morin transition, with no indication of a Verwey transition. Therefore, we used the pure mineral values of $M_s$ for weighting in the calculations. For two out of the three mixtures, linear additivity is fairly well verified (Fig. 11). The mixtures of magnetite M4000 and hematite made from M4000 does not obey linear additivity (Fig. 11a) whereas the other two mixtures do (Fig. 11b and c), over the given range.

## 5. Discussion

### 5.1. Comparison with other studies

Our results are in good agreement with the results of Muxworthy et al. (2005), who found that mixtures of soft minerals like magnetite can exhibit non-linear behaviour because of possible magnetostatic interactions. The results of the modelling from this study confirms that non-linearity is a result of the interactions. They also found that mixtures of a hard and a soft phase add linearly up a critical concentration, and that hematite could be seen on a FORC diagram when the concentration of magnetite was no more than 81%, which is in reasonable agreement with our limit of 88%.

It is well accepted that non-interacting mixtures have linearly additive magnetizations. For example, Carter-Stiglitz et al. (2001) argued that their experiments were unaffected by interactions because they used components that were dispersed (0.1% magnetite by weight) in a magnetically clean diamagnetic matrix. Their definition of linear additivity was the same as ours: they found that hysteresis loops can effectively predict mixing ratios in mixtures of SD/SP, SD/MD and SP/MD grains.

Lees (1997) demonstrated non-linearity as a function of mixing ratio for many of her samples. However, her results are not necessarily in conflict with ours. One factor that could have caused the non-linear behaviour in the study by Lees (1997) is the change in interaction state between the pure end-members and the mixtures: the undiluted end-members probably suffered from interaction effects before being dispersed in the mixture; once the end-members were diluted in the mixtures, the interaction effects would be reduced. In our case, the mixed samples and the end-member samples were prepared in exactly the same way, with the same bulk concentration in matrix and the same degree of actual dispersion, so the interaction state should stay the same for different mixing ratios, including 100%. This might explain why linear additivity is still observed in our measurements, even when magnetic grain concentration is as high as 10%.

It is also difficult to know the interaction state in a mixture. In our case, we assumed that the mixtures used in the measurements are interacting, based on the spread of the FORC distribution in the $H_u$ direction and the relatively high particle concentrations. It might also be possible that the interactions present in the experimental samples were not high enough to compromise linear additivity. Even though results from the modelling and the measurements are consistent, it has to be kept in mind that in the modelling we studied assemblages of SD grains, whereas the grain size/domain state of the measured samples is much more diverse and goes from SD to PSD.

### 5.2. Hematite–magnetite mixtures

When assessing the linear additivity of FORCs of hematite–magnetite mixtures, each component has to be weighted to take into account the large difference in $M_S$ values for the two minerals. Therefore, the hematite contribution will not be detected for proportions of magnetite that are too large (larger than 12% according to our measurements) and its presence will not be predicted by the linear fitting of FORCs. The linear additivity is not a surprise, because in mixtures containing only one hard magnetic mineral (hematite in our case), which has a reduced anisotropy $(2K)/M_S$ much larger than that of magnetite, there are negligible magnetostatic interactions between the phases. The response of hematite to the interaction field of magnetite is dictated by anisotropy. In the other direction, the $M_S$ vector for magnetite is not affected much by the interaction field of hematite during hysteresis because its small $M_S$ creates a small interaction field. The large difference in saturation magnetizations between magnetite and hematite means that the magnetic energy stored in magnetite is large compared to hematite. For example, in a mixture with 1% by mass of magnetite, the energy in terms of $M_S$ is three times that of 99% hematite by mass. In the experimental mixtures, the magnetite FORC peak is much higher than that of hematite and it is also much sharper. However, the sharpness of the peak is not obvious from the FORC diagrams because of the high SF of five.

Even concentrated hematite–magnetite mixtures will have linearly additive FORC distributions. However, our results suggest that FORC diagram measurements, like hysteresis loops, are not an ideal method for identifying hematite in mixtures dominated by magnetite, or any other strongly magnetic mineral. Low-temperature remanence methods are much more appropriate, because the usual SD state of hematite magnifies its remanent signal.

### 5.3. Reproducibility of FORC diagrams

To address the question of the experimental reproducibility of FORC diagrams and confidence intervals on the contours, we measured a basalt sample (originally part of another study) 10 times, without changing the orientation of the sample. This gives the noise level created by the machine. We find that the standard deviation on each point of the FORC distribution is on

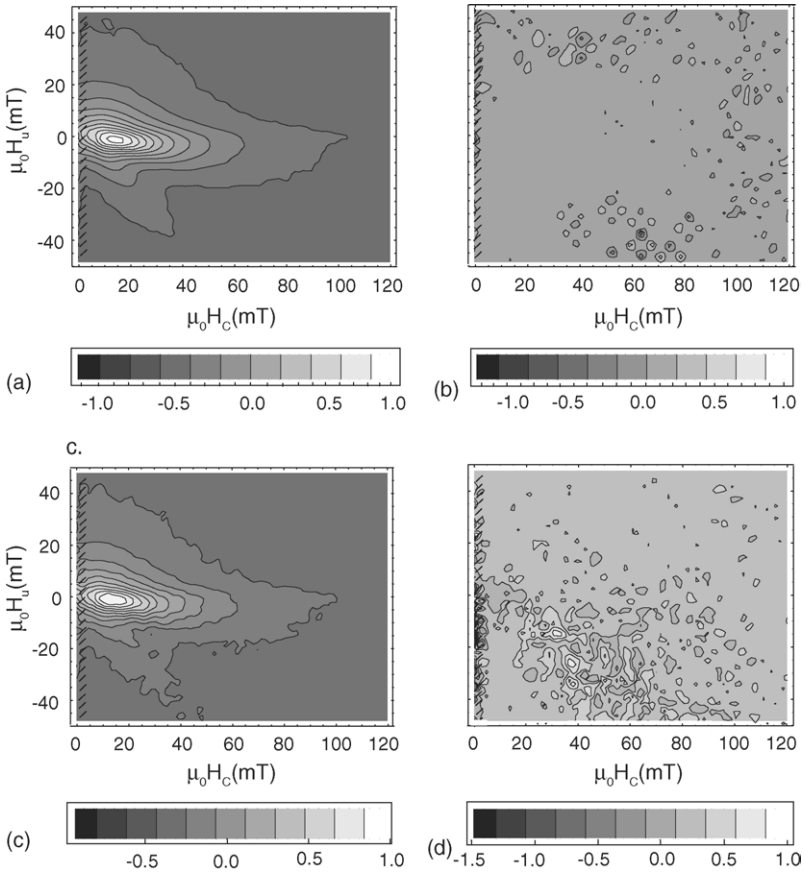


Fig. 12. Average of the 10 replicated FORC distributions (a and c) and point-by-point standard deviations of the 10 replicated FORC distributions (b and d) for FORCs measured on the same sample—top: in the same orientation; bottom: in different orientations. The distributions are normalized to their maximum values.

average 0.2% of the value. Moreover, the standard deviation is larger in the region close to the vertical axis, where data are extrapolated, and on the sides of the diagram, where the distribution is small (Fig. 12a and b). The standard deviation is smallest in the region of interest. We also measured the same sample 10 times, but in different orientations with rotation of the sample between the 10 measurements (Fig. 12c and d). Now, the average ratio of the standard deviation over the FORC value is 1.7%. Again, most of standard deviation distribution is concentrated along the $H_c = 0$ axis and along the line 45° of the horizontal axis. These results indicate that in the region of interest, the FORC distribution has a good reproducibility.

### 5.4. Negative regions on FORC diagrams

Negative asymmetrical regions on FORC diagrams have been observed in many FORC studies. Almost all of our FORC diagrams contain a negative region. They have two different origins. A broad negative peak is present on almost all FORC diagrams of samples containing a significant fraction of hematite (Fig. 10a). Negative peaks are also visible in nearly all of the bimodal magnetite mixture models. In this case, the negative peak is always centered at $H_c = 0$, $H_u = -H_C$, $H_C$ being the coercivity peak. This region corresponds to the FORCs with a reversal field $H_a$ close to the coercive force $H_C$ and $H_b$ slightly larger than $H_a$. In this region, $\partial M/\partial H_b$ decreases with decreasing $H_a$, causing $\rho(H_a, H_b)$ to be negative (Muxworthy et al., 2004). This negative region is real and is not an artifact of the data processing procedure.

## 6. Implications

This study has several applications for environmental magnetism and paleomagnetism. First, the micromagnetic model confirms that magnetic interactions between magnetite grains are easily visible on a FORC diagram. The spreading of the FORC distribution along the $H_u$

axis stays constant when $d$ is decreased from 5 to 3, then increases slightly when $d$ is between 3 and 2, and finally increases dramatically when $d$ is further reduced.

We also investigated the efficiency of the FORC method to detect hematite in a mixture with magnetite, and to predict the correct mixing ratios, compared to two other methods. First, FORCs are a more effective way of predicting mixing ratios than major hysteresis curves. Major loops fail more often than FORC diagrams to predict the correct mixing ratios, particularly for non-interacting or weakly interacting mixtures. This is not surprising because FORC diagrams contain about two orders of magnitude more data than major hysteresis loops. Using the major hysteresis loop and low-temperature data, Carter-Stiglitz et al. (2001) designed a singular-value decomposition to solve for the various proportions of the magnetic phases in mixtures. They proved the efficiency of the method with several examples. The drawback of their technique is that it requires both hysteresis data and low-temperature SIRM curves. While hysteresis loops are much faster to acquire than FORC diagrams, low-temperature measurements are usually more time consuming and require two sets of specialized instrumentation not available in most laboratories.

Detecting hematite in mixtures with high $M_S$ minerals using FORC diagrams is not straightforward. While FORC diagrams can predict the correct proportion of hematite in a mixture in which it is known that hematite is present, FORC diagrams are not the most efficient way of identifying the presence of hematite in a completely unknown sample. Low-temperature SIRM curves can do this in a much more convincing way. Even by increasing the number of contours, the minimum concentration of hematite that can still be detected in the experimental mixtures containing magnetite is about 88%, while low-temperature SIRM curves can detect as little as 50% hematite mixed with magnetite.

## 7. Conclusions

1. FORC diagrams were modelled micromagnetically for different assemblages of SD magnetite with a bimodal distribution of coercivities, and using various spacings between grains in each assemblage. After fitting FORCs of mixtures with a combination of the end-member FORCs, predicted mixing ratios were within 8% of the actual mixing ratios for weakly interacting and non-interacting regimes.
2. Experimental measurements of FORC diagrams support the conclusion from our modelling. Most of the bimodal mixtures of magnetite (SD + PSD) have FORC diagrams that are linearly additive within the error bars. For the 10% concentration mixtures, 10 out of 13 predicted mixing ratios were in agreement with the actual ratios, and only one was more than 8% different.
3. Linear additivity of the two end-members holds in FORC diagrams of mixtures of SD magnetite and SD hematite. However, the small $M_S$ of hematite compared to that of magnetite makes it difficult to detect a contribution from hematite on a FORC diagram unless it comprises ≈90% or more of the mixture, and unless the number of contours plotted on the FORC diagram is increased above 10. FORC diagrams are not well suited to the detection of small quantities of weakly magnetic minerals mixed with strongly magnetic minerals. SIRM warming and cooling curves are much more effective in detecting weakly magnetic minerals.
4. According to our micromagnetic modelling, magnetic interactions can begin to be detected in FORC diagrams when $d$ is smaller than 3, which corresponds to a concentration of 1.5%, and more clearly when $d$ is 2 or less, corresponding to a 5% concentration.

## Acknowledgments

We are grateful to Özden Özdemir for advice and assistance with the experimental samples. FORC measurements of mixtures of magnetite and hematite were carried out at the Institute for Rock Magnetism, which is supported by the University of Minnesota, the Keck Foundation, and the NSF Earth Sciences Division. We thank Mike Jackson, Jim Marvin and Peat Solheid for helping with the measurements. Brian Carter-Stiglitz and Mark Dekkers provided helpful reviews. This research was supported by NSERC Canada grant A7709 to D.J.D.

## References

Bloemendal, J., Barton, C.E., Radhakrishnamurthy, C., 1985. Correlation between Rayleigh loops and frequency-dependent and quadrature susceptibility. J. Geophys. Res. 90, 8789–8792.

Carter-Stiglitz, B., Moskowitz, B., Jackson, M., 2001. Unmixing magnetic assemblages and the magnetic behavior of bimodal mixtures. J. Geophys. Res. 106, 26397–26411.

Carvallo, C., Muxworthy, A.R., Dunlop, D.J., Williams, W., 2003. Micromagnetic modelling of first-order reversal curve (FORC) diagrams for single-domain and pseudo-single-domain magnetite. Earth Planet. Sci. Lett. 213, 375–390.

Carvallo, C., Özdemir, Ö., Dunlop, D.J., 2004. First-order reversal curve (FORC) diagrams of elongated single-domain grains at high and low temperatures. J. Geophys. Res. 109, 04105.

Day, R., Fuller, M., Schmidt, V.A., 1977. Hysteresis properties of titanomagnetites: grain size and compositional dependence. Phys. Earth Planet. Inter. 13, 206–267.

Dunlop, D.J., Özdemir, Ö., 1997. Rock Magnetism: Fundamentals and Frontiers. Cambridge Univ. Press, Cambridge and New York 573 pp.

Dunlop, D.J., Argyle, K.S., 1991. Separating multidomain and single-domain-like remanences in pseudo-single-domain magnetites (215–540 nm) by low-temperature demagnetization. J. Geophys. Res. 96, 2007–2017.

Dunlop, D.J., 2002. Theory and application of the Day plot ($M_{rs}/M_s$ versus $H_{cr}/H_c$) 1. Theoretical curves and tests using titanomagnetite data. J. Geophys. Res. 107 (B3), 2056 doi:10.1029/2001JB00486 EPM 4–1 to 4–22.

Efron, B., Tibshirani, R.J., 1993. An Introduction to the Bootstrap. Chapman and Hall, New York 456 pp.

Fletcher, E.J., O'Reilly, W., 1974. Contribution of $Fe^{2+}$ ions to the magnetocrystalline anisotropy constant $K_1$ of $Fe_{3-x}Ti_xO_4$ ($0 < x < 0.1$). J. Phys. C.: Solid State Phys. 7, 171–178.

Lees, J.A., 1997. Mineral magnetic properties of mixtures of environmental and synthetic materials: linear additivity and interaction effects. Geophys. J. Int. 131, 335–346.

Muxworthy, A., Williams, W., Virdee, D., 2003. The effect of magnetostatic interactions on the hysteresis parameters of single-domain and pseudo-single-domain grains. J. Geophys. Res. 108, 2517.

Muxworthy, A.R., Heslop, D., Williams, W., 2004. Influence of magnetostatic interactions on first-order-reversal-curve (FORC) diagrams: a micromagnetic approach. Geophys. J. Int. 158, 888–897.

Muxworthy, A.R., Williams, W., 2005. Magnetostatic interaction fields in first-order-reversal-curve (FORC) diagrams. J. Appl. Phys. 97, 063905.

Muxworthy, A.R., King, J.G., Heslop, D., 2005. Assessing the ability of first order reversal curve (FORC) diagrams to unravel complex magnetic signals. J. Geophys. Res. 110, B01105.

Pauthenet, R., Bochirol, L., 1951. Aimantation spontanée des ferrites. J. Phys. Rad. 12, 249–251.

Pike, C.R., Roberts, A.P., Verosub, K.L., 1999. Characterizing interactions in fine magnetic particle systems using first order reversal curves. J. Appl. Phys. 85, 6660–6667.

Roberts, A.P., Cui, Y.L., Verosub, K.L., 1995. Wasp-waisted hysteresis loops: mineral magnetic characteristics and discrimination of components in mixed magnetic systems. J. Geophys. Res. 100, 17909–17924.

Roberts, A.P., Pike, C.R., Verosub, K.L., 2000. First-order reversal curve diagrams: a new tool for characterizing the magnetic properties of natural samples. J. Geophys. Res. 105, 28461–28475.

Stancu, A., Pike, C.R., Stoleriu, L., 2003. Micromagnetic and Preisach analysis of the first order reversal curve (FORC) diagram. J. Appl. Phys. 93, 6620–6622.

Stoner, E.C., Wohlfarth, E.P., 1948. A mechanism of magnetic hysteresis in heterogeneous alloys. Phil. Trans. Roy. Soc. London A240, 599–642.

Tauxe, L., Mullender, T.A.T., Pick, T., 1996. Potbellies, wasp-waists, and superparamagnetism in magnetic hysteresis. J. Geophys. Res. 101, 571–593.

van Oorschot, I.H.M., Dekkers, M.J., 1999. Dissolution behaviour of fine-grained magnetite and maghemite in the citrate-bicarbonate-dithionite extraction method. Earth Planet. Sci. Lett. 167, 283–295.

Weaver, R., Roberts, A.P., Barker, A.J., 2002. A late diagenetic (syn-folding) magnetization carried by pyrrhotite: implications for palaeomagnetic studies from magnetic iron sulphide-bearing sediments. Earth Planet. Sci. Lett. 200, 371–386.

Wright, T.M., Williams, W., Dunlop, D.J., 1997. An improved algorithm for micromagnetics. J. Geophys. Res. 102, 12085–12094.

Yu, Y., Dunlop, D.J., Özdemir, Ö., 2002. Partial anhysteretic remanent magnetization in magnetite. 1. Additivity. J. Geophys. Res. 107, 2244.